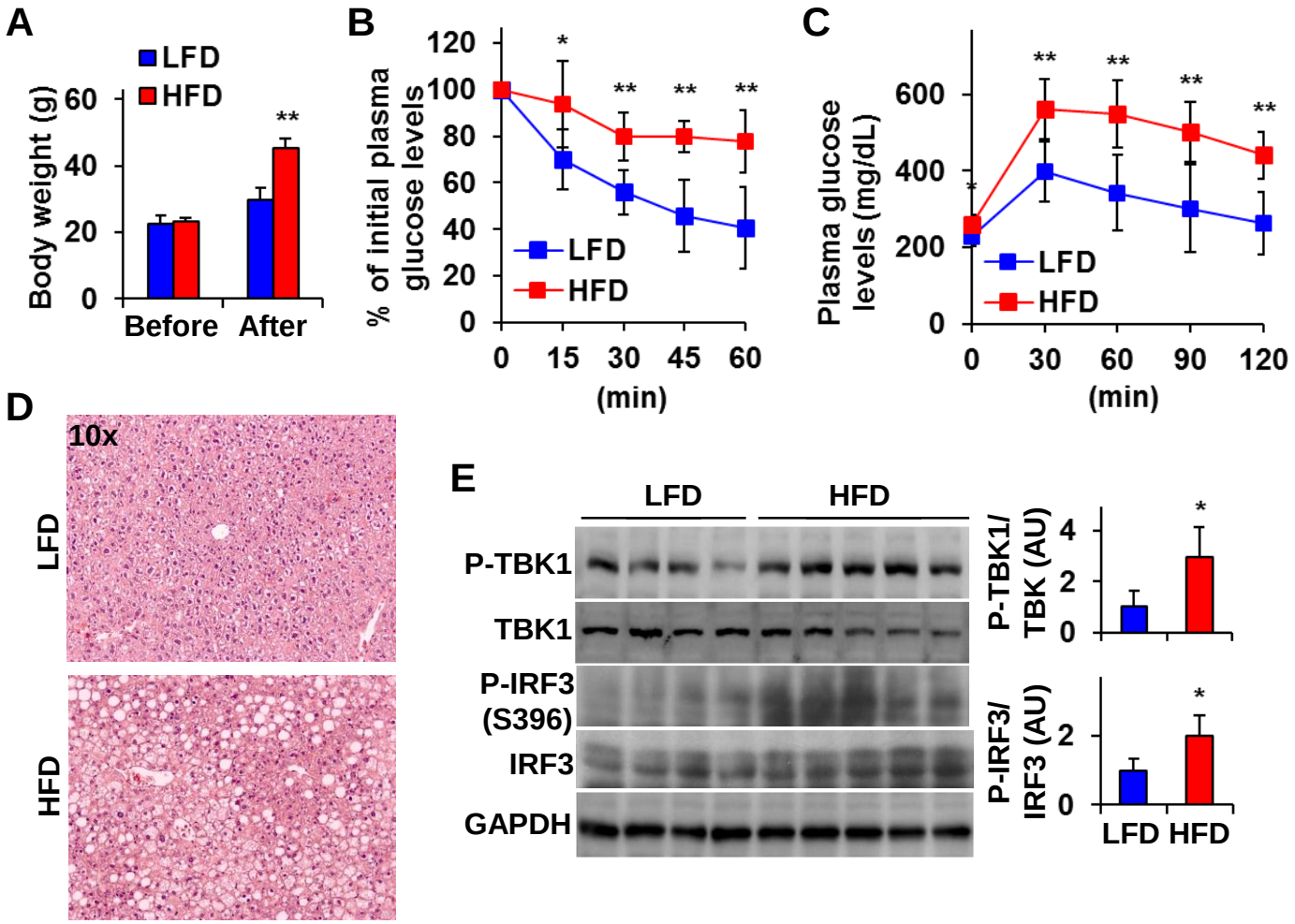

Figure S1. **HFD feeding increases liver signaling events downstream of STING while inducing insulin resistance, glucose intolerance, and NAFLD**

Male C57BL/6J mice, at 5 - 6 weeks of age, were fed a high-fat diet (HFD) or low-fat diet (LFD) for 12 weeks. (**A**) Body weight was monitored before and after the feeding period. (**B**, **C**) Insulin (B) and glucose (C) tolerance tests. After the feeding period, mice were fasted for 4 hr and received an intraperitoneal injection of insulin (1 U/kg) and glucose (2 g/kg), respectively. (**D**) Liver sections were stained with H&E. (**E**) Liver signaling events downstream of STING. Liver lysates were examined for total and phosphorylated TBK1 and IRF3. Bar graphs, quantification of blots. AU, arbitrary unit. For A - C, and E, numeric data are means ± SD. n = 10 - 12 (A - C) or 6 - 7 (E). *, $P < 0.05$ and **, $P < 0.01$ HFD vs. LFD in A for mice after dietary feeding, in B and C for the same time point, or in E.

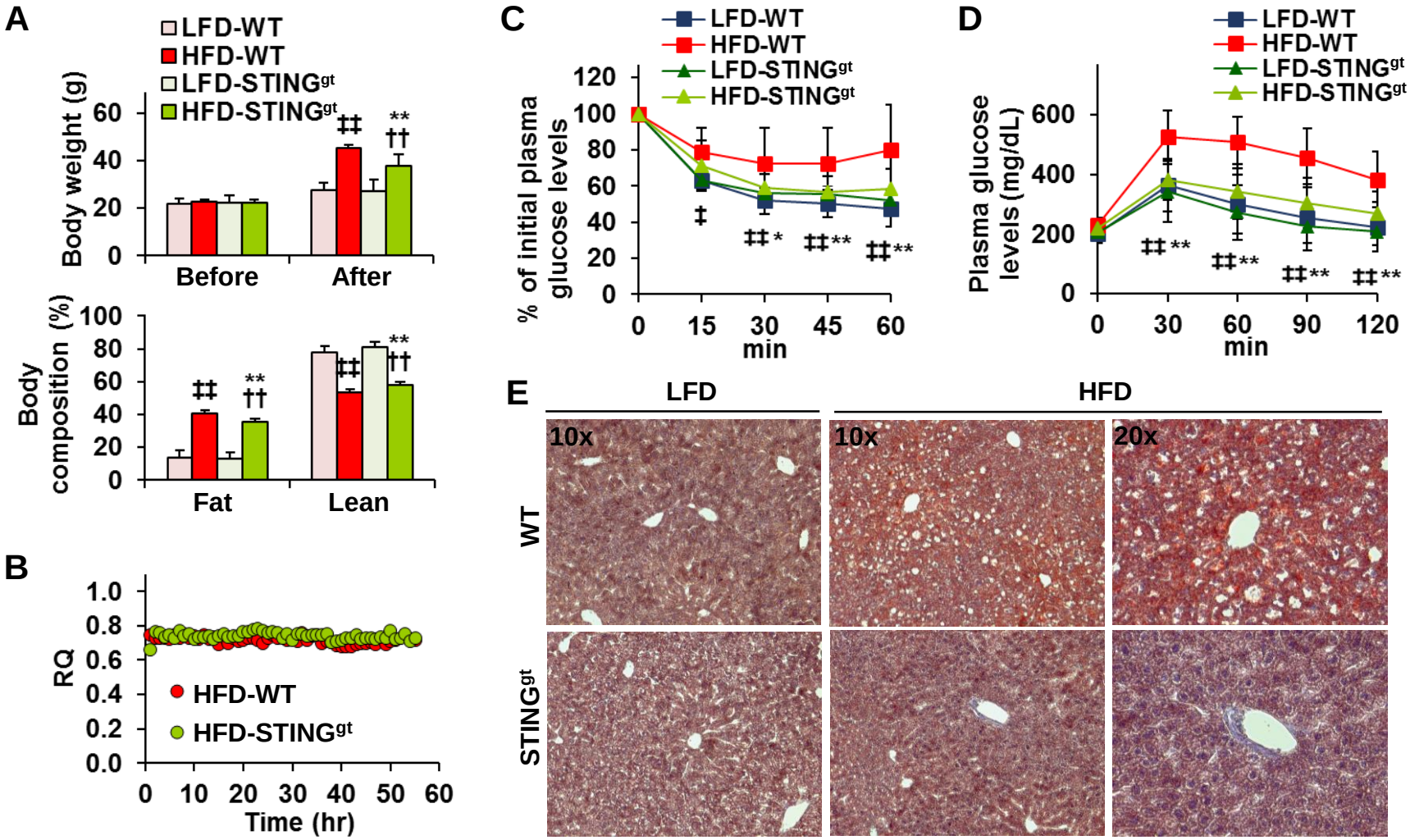

Figure S2. **Related to Figure 2: STING disruption protects against HFD-induced obesity and NAFLD**

Male STING-disrupted (STING^{gt}) (C57BL/6J background) mice and wild-type (WT) C57BL/6J mice, at 5 - 6 weeks of age, were fed as described in Fig. S1. (**A**) Top panel, body weight was recorded before and after the feeding period; bottom panel, body composition was analyzed using EchoMRI after feeding period. (**B**) Respiratory quotient (RQ). After the feeding period, mice were subjected to the Promethion^{TM} system to measure energy metabolism. (**C**,**D**) Insulin (C) and glucose (D) tolerance tests. After the feeding period, mice were fasted for 4 hr and received an intraperitoneal injection of insulin (1 U/kg) and glucose (2 g/kg), respectively. For A - D, data are means ± SD. n = 10 - 12 (in A, C, and D) or 8 (in C). *, $P < 0.05$ and **, $P < 0.01$ HFD-STING^{gt} vs. HFD-WT in A after the feeding period or for the same type of mass or in C and D for the same time point; ‡, $P < 0.05$ and ‡‡, $P < 0.01$ HFD-WT vs. LFD-WT in A after feeding period or for the same type of mass or in C and D for the same time point; ††, $P < 0.01$ HFD-STING^{gt} vs. LFD-STING^{gt} in A after the feeding period or for the same type of mass. (**E**) Liver sections were stained with oil red O.

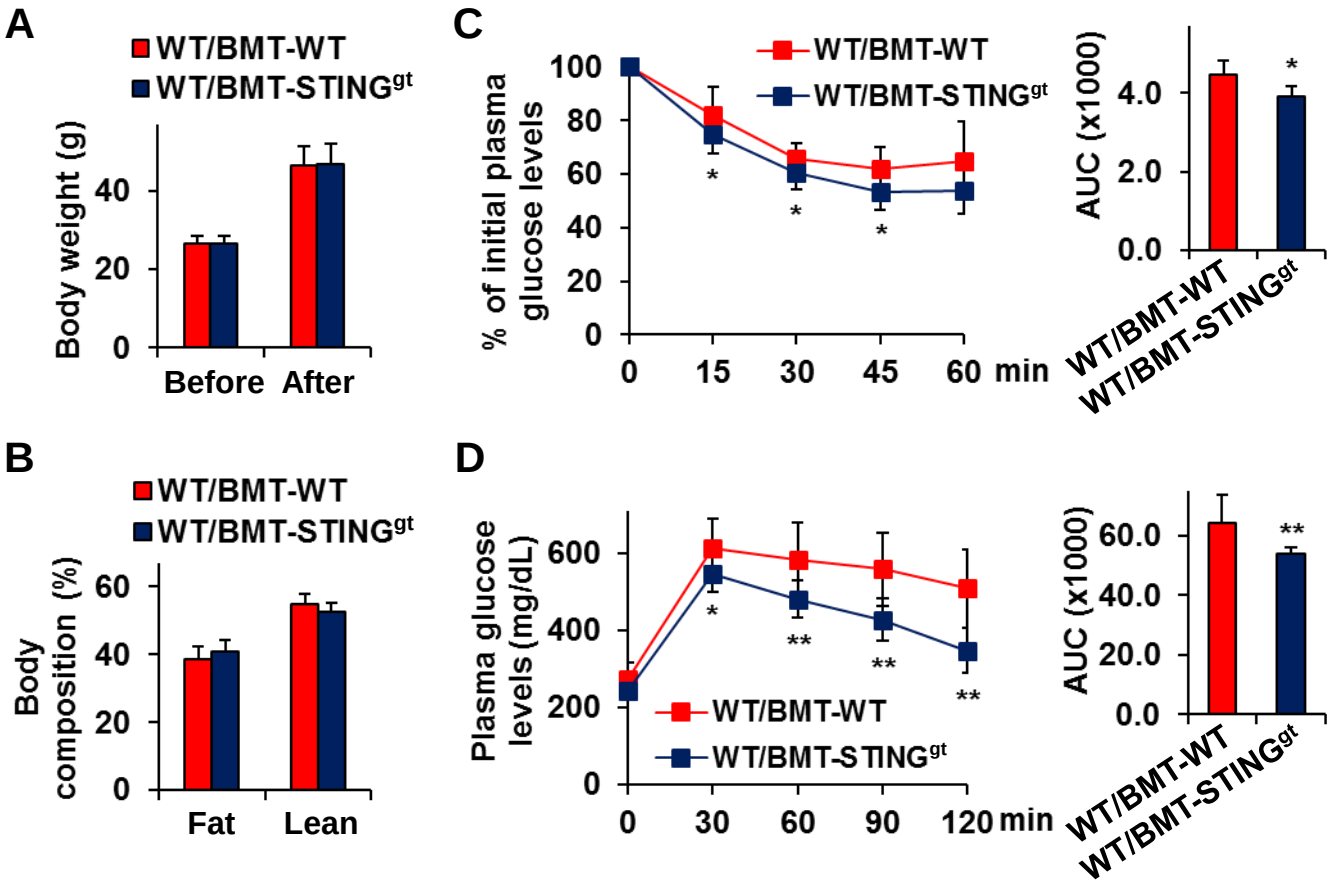

Figure S3. **Related to Figure 3: Myeloid cell-specific STING disruption decreases the severity of HFD-induced NAFLD**

Male WT C57BL/6J mice, at 5 - 6 weeks of age, were lethally irradiated and transplanted with bone marrow cells from STING^{gt} and/or WT mice. After recovery for 4 weeks, the chimeric mice were fed an HFD for 12 weeks. WT/BMT-STING^{gt}, WT mice received STING^{gt} bone marrow cells; WT/BMT-WT, WT mice received WT bone marrow cells. (**A**) Body weight was recorded before and after the feeding period. (**B**) Body composition. (**C**,**D**) Insulin (C) and glucose (D) tolerance tests. After the feeding period, mice were fasted for 4 hr and received an intraperitoneal injection of insulin (1 U/kg) and glucose (2 g/kg), respectively. AUC, area under curve. For A - D, data are means ± SD. n = 9 - 12. *, $P < 0.05$ and **, $P < 0.01$ WT/BMT-STING^{gt} vs. WT/BMT-WT in bar graphs of C and D or in line graphs of C and D for the same time point.

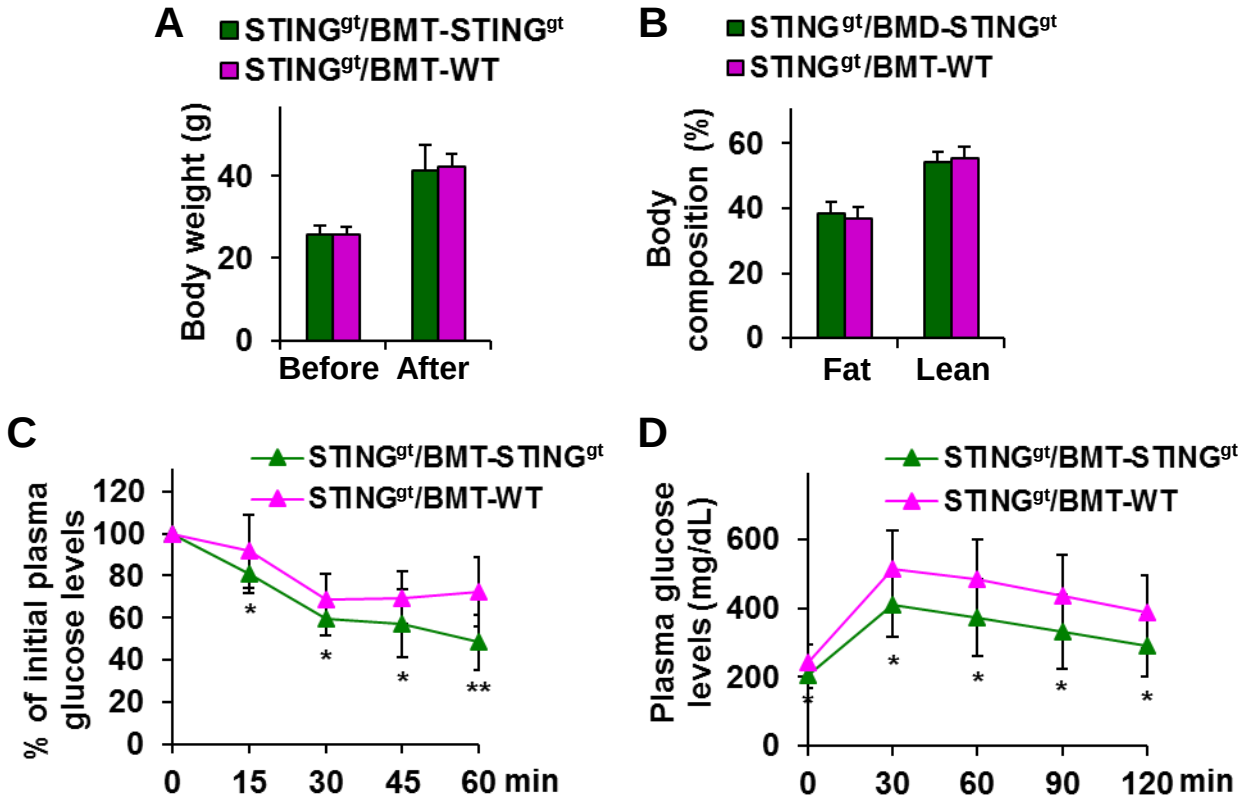

Figure S4. **Related to Figure 4: Myeloid cell-specific STING presence exacerbates HFD-induced NAFLD**

Male STING^{gt} mice, at 5 - 6 weeks of age, were lethally irradiated and transplanted with bone marrow cells from WT and/or STING^{gt} mice. After recovery for 4 weeks, the chimeric mice were fed an HFD for 12 weeks. STING^{gt}/BMT-WT, STING^{gt} mice received WT bone marrow cells; STING^{gt}/BMT-STING^{gt}, STING^{gt} mice received STING^{gt} bone marrow cells. (**A**) Body weight was recorded before and after the feeding period. (**B**) Body composition. (**C**,**D**) Insulin (C) and glucose (D) tolerance tests. After the feeding period, mice were fasted for 4 hr and received an intraperitoneal injection of insulin (1 U/kg) (C) and glucose (2 g/kg) (D), respectively. For A - D, data are means ± SD. n = 10 - 12. *, $P < 0.05$ and **, $P < 0.01$ STING^{gt}/BMT-WT vs. STING^{gt}/BMT-STING^{gt} in C and D for the same time point.

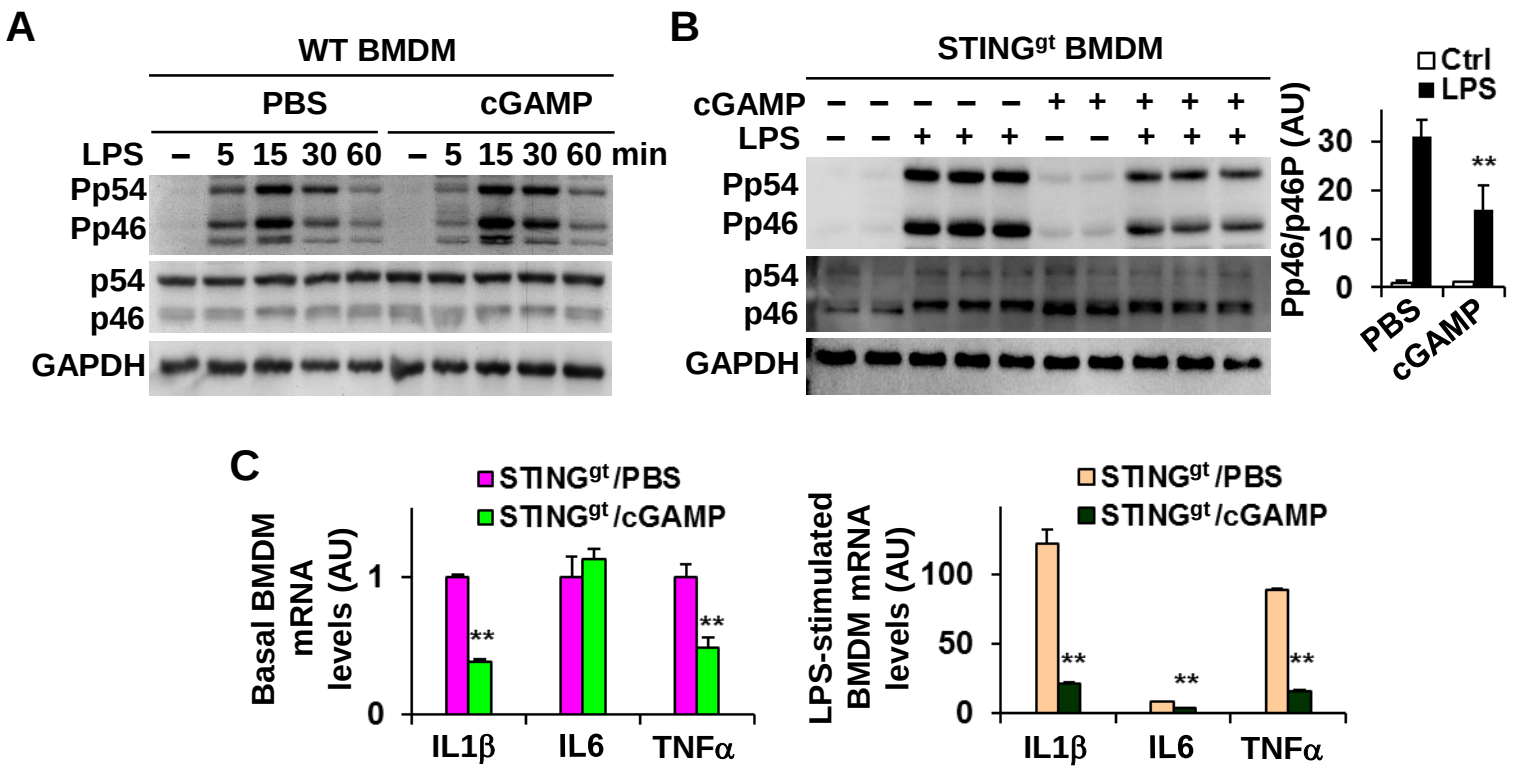

Figure S5. **Related to Figure 5: STING regulates macrophage inflammatory activation**
Bone marrow cells were isolated from male STING^{gt} mice and WT mice, at 11- 12 weeks of age. After differentiation, bone marrow-derived macrophages (BMDM) were treated with or without cGAMP (20 ng/mL) for 24 hr in the absence or presence of LPS (100 ng/mL) for the indicated time period (A) or for 30 min (B) prior to harvest to analyze inflammatory signaling or LPS (20 ng/mL) for 6 hr prior to harvest to analyze cytokine expression. (**A**,**B**) Cell lysates were examined for JNK p46 signaling using Western blot analysis. Bar graph in B, quantification of blots. (**C**) Macrophage cytokine expression was analyzed using real-time RT-PCR. For B and C, numeric data are means ± SD. n = 4 - 6. **, $P < 0.01$ cGAMP vs. PBS under LPS-stimulated condition (in B) or STING^{gt}/cGAMP vs. STING^{gt}/PBS for the same gene (in C).

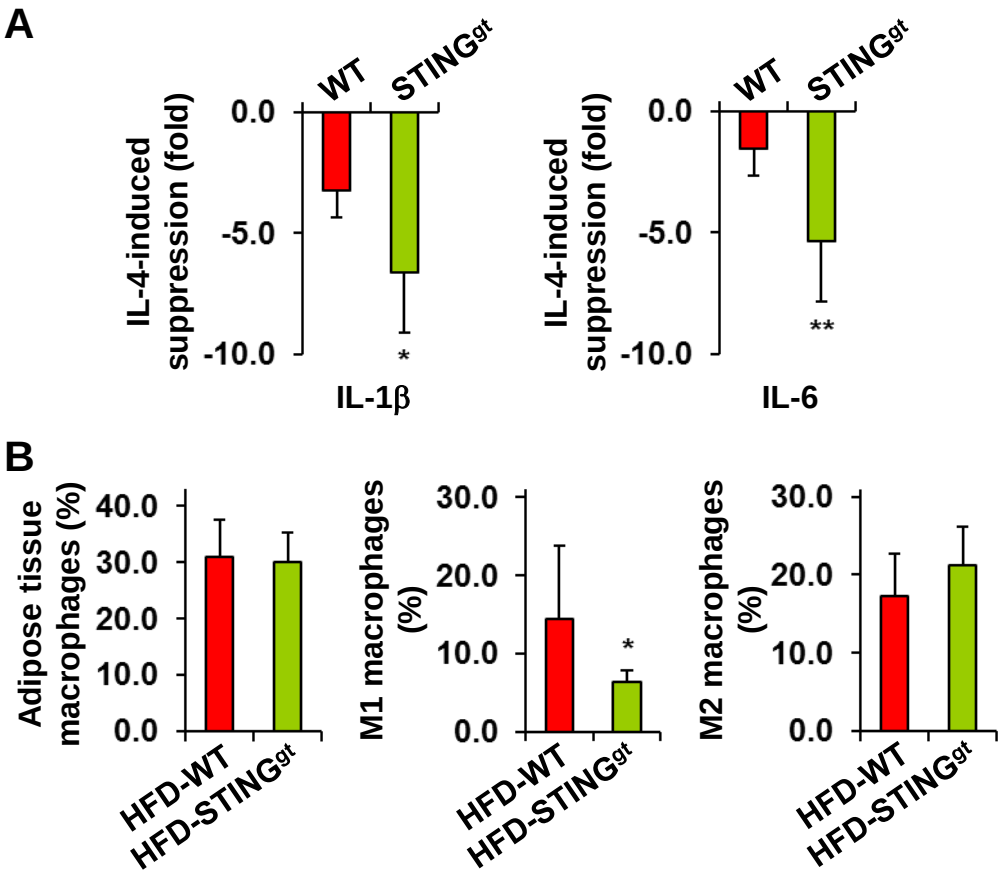

Figure S6. **Related to Figure 5: STING regulates macrophage polarization**

(**A**) Macrophage alternative activation. BMDM were prepared as described in Figure S5. Prior to harvest, BMDM were treated with or without interleukin 4 (IL-4, 10 ng/mL) for 48 hr. Macrophage cytokine expression was analyzed using real-time RT-PCR. The mRNA levels of IL-1β and IL-6 were presented as folds of suppression upon IL-4 induction. (**B**) Adipose tissue macrophage infiltration and polarization. Mice were fed as described in Figure S2. After the feeding period, mice were fasted for 4 hr prior to harvest. Stromal vascular cells (SVC) were isolated from adipose tissue and analyzed for CD11b and F4/80 expression (maturate macrophages). Mature macrophages were further analyzed for CD11c and CD206 expression. Left panel, percentages of mature macrophages ($F4/80^+$ $CD11b^+$ cells); middle panel, percentages of M1 macrophages ($F4/80^+$ $CD11b^+$ $CD11c^+$ $CD206^-$ cells); right panel, percentages of M2 macrophages ($F4/80^+$ $CD11b^+$ cells $CD11c^-$ $CD206^+$ cells). For A and B, data are means ± SD. n = 6 (A) or n = 10 - 12 (B).). *, $P < 0.05$ and **, $P < 0.01$ $STING^{gt}$ vs. WT in A or HFD-$STING^{gt}$ vs. HFD-WT in B.

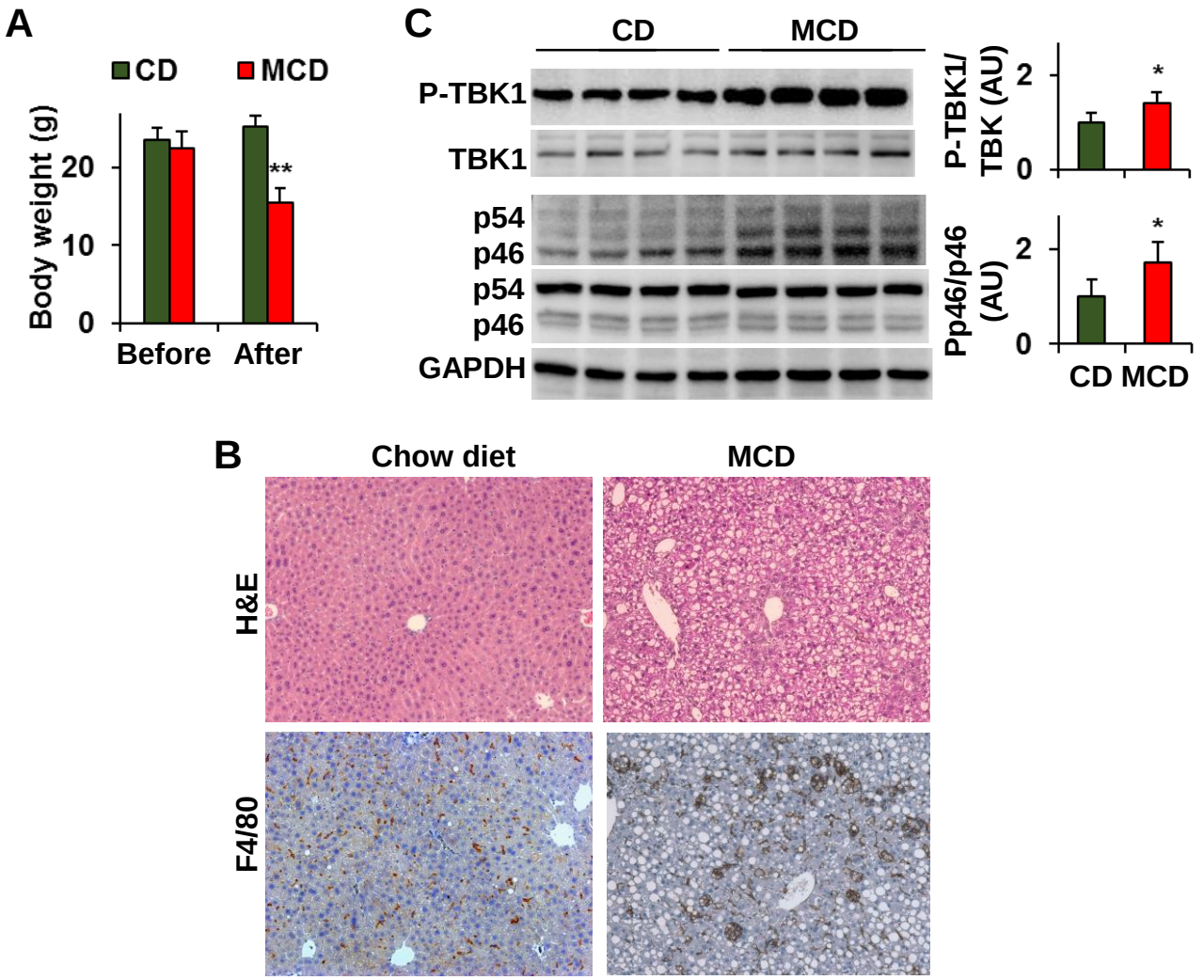

Figure S7. **Related to Figure 6: MCD feeding increases liver TBK1 phosphorylation while inducing steatohepatitis**

Male C57BL/6J mice, at 11 - 12 weeks of age, were fed a methionine- and choline-deficient diet (MCD) or 5 weeks or maintained on a chow-diet (CD). (**A**) Body weight was monitored before and after the feeding period. (**B**) Liver sections were stained with H&E (top row) or stained for F4/80 expression (bottom row). (**C**) Liver phosphorylation states of TBK1 and JNK p46. Liver lysates were examined for total and phosphorylated TBK1 and JNK p46. Bar graphs, quantification of blots. For bar graphs in A and C, data are means ± SD. n = 11 - 13 (A) or 6 - 8 (C). *, $P < 0.05$ and **, $P < 0.01$ MCD vs. CD in A for mice after dietary feeding or in C.

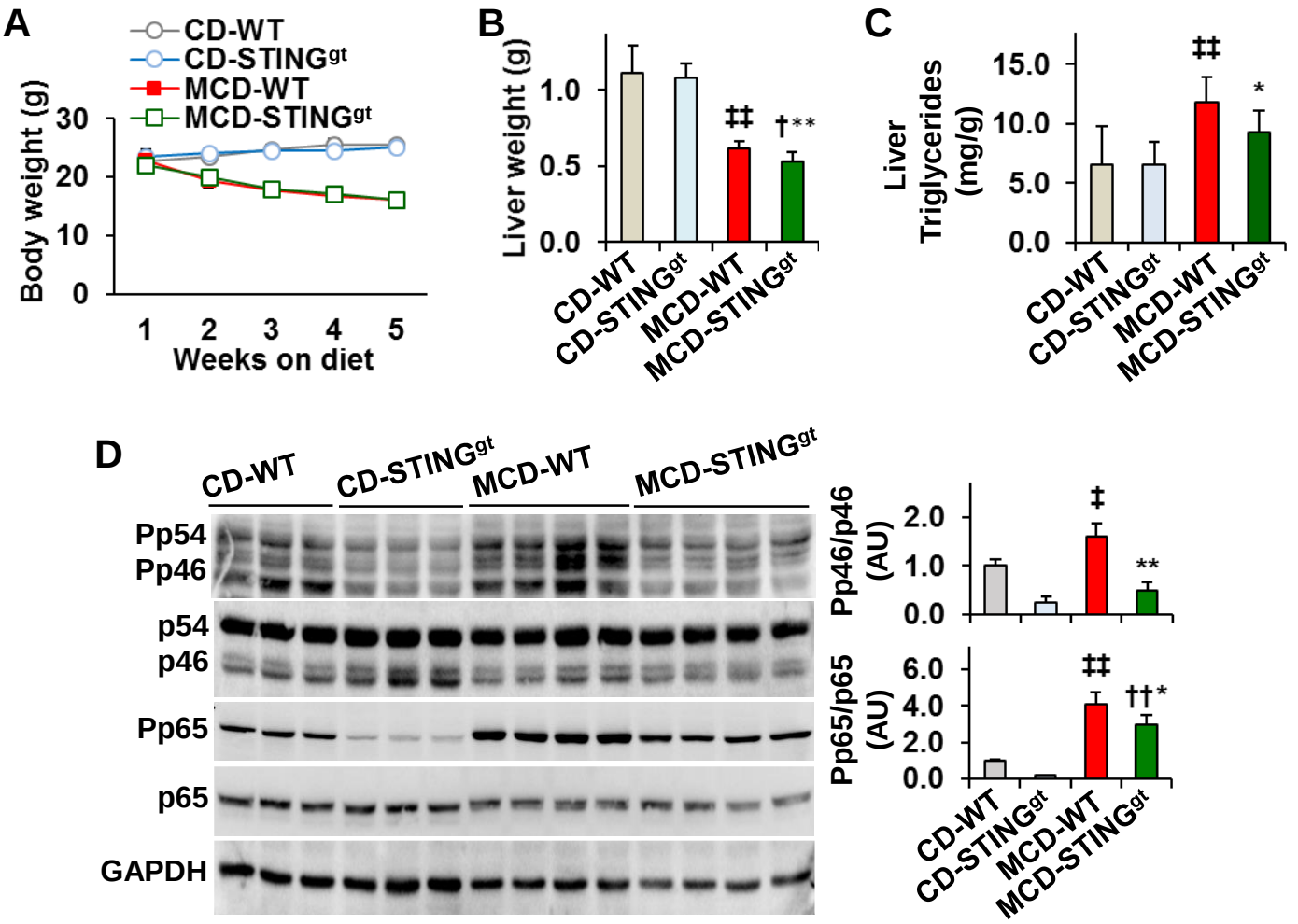

Figure S8. **Related to Figure 6: STING disruption decreases the severity of MCD-induced steatohepatitis**

Male STING^{gt} mice and WT mice, at 11- 12 weeks of age, were fed a methionine- and choline-deficient diet (MCD) or 5 weeks or maintained on a chow-diet (CD). (**A**) Body weight was monitored during the feeding period. (**B**) Liver weight. After the feeding period, mice were fasted for 4 hr prior to harvest. (**C**) Liver levels of triglycerides. (**D**) Liver inflammatory signaling. Liver lysates were examined for total and phosphorylated JNK p46 and NFκB p65. Bar graphs, quantification of blots. For A - D, numeric data are means ± SD. n = 8 - 10 (A - C) or 6 - 8 (D). *, $P < 0.05$ and **, $P < 0.01$ MCD-STING^{gt} vs. MCD-WT; ‡, $P < 0.05$ and ‡‡, $P < 0.01$ MCD-WT vs. CD-WT; †, $P < 0.05$ and ††, $P < 0.01$ MCD-STING^{gt} vs. CD-STING^{gt}. Data of MCD-fed mice in Figure S8B and S8C are also presented in Figure 6B and 6C, respectively.

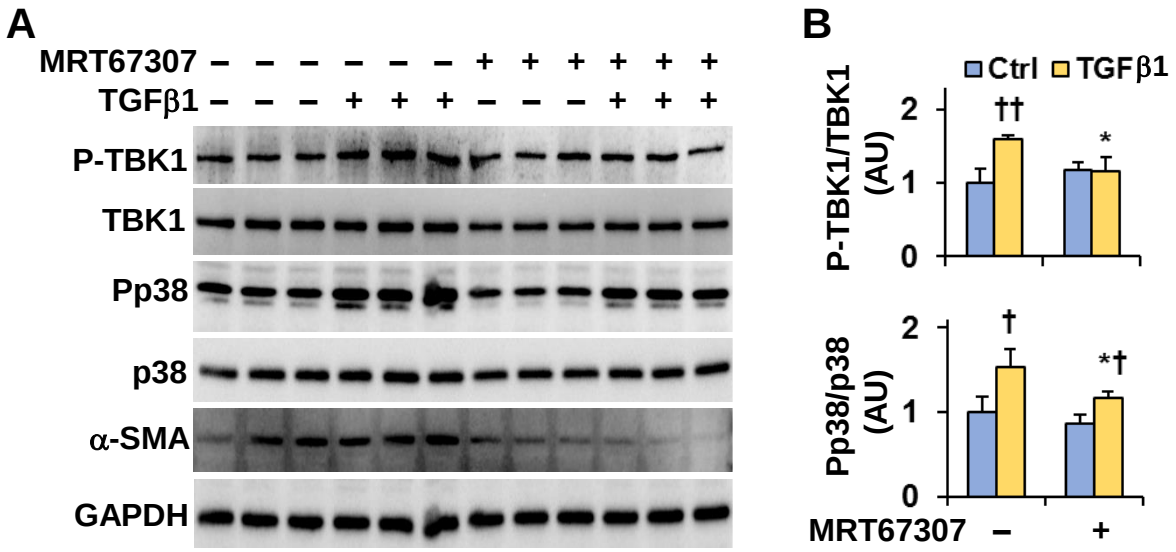

Figure S9. **Related to Figure 7: TBK1 inhibition decreases HSC activation**
LX2 cells were treated with MRT67307 (TBK1 inhibitor) (1 μM) in the absence or presence of TGFβ1 (8 ng/mL) for 24 hr. (**A**) TBK1 phosphorylation and HSC activation. Cell lysates were subjected to Western blot analysis. (**B**) Quantification of blots. Data are means ± SD. n = 6. *, $P < 0.05$ MRT67307 vs. Control (in the absence of MRT) for TGFβ1-treated cells; †, $P < 0.05$ and ††, $P < 0.01$ TGFβ1 vs. Ctrl under the same condition (with or without MRT).

Expression on STING Is Increased in Liver Tissues from Patients with NAFLD and Promotes Macrophage-mediated Hepatic Inflammation and Fibrosis in Mice

Xianjun Luo[1*], Honggui Li[1*], Linqiang Ma[1,2,3*], Jing Zhou[1], Xin Guo[1], Shih-Lung Woo[1], Ya Pei[1], Linda R. Knight[4], Michael Deveau[4], Yanming Chen[5], Xiaoxian Qian[6], Xiaoqiu Xiao[2], Qifu Li[3], Xiangbai Chen[7], Yuqing Huo[8], Kelly McDaniel[9,10], Heather Francis[9,10], Shannon Glaser[9,10], Fanyin Meng[9], Gianfranco Alpini[9,10†], and Chaodong Wu[1†]

[1] Department of Nutrition and Food Science, Texas A&M University, College Station, TX 77843, USA,

[2] Department of Endocrinology and [3] the Laboratory of Lipid & Glucose Metabolism, the First Affiliated Hospital of Chongqing Medical University, Chongqing 400016, China;

[4] Radiation Oncology, Veterinary Medical Teaching Hospital, Texas A&M University, College Station, TX 77843, USA,

[5] Department of Endocrinology and [6] Department of Cardiology, the Third Affiliated Hospital of Sun Yat-sen University, Guangzhou, Guangdong 510630, China;

[7] Pathology, Baylor Scott & White Health, College Station, TX 77845; USA

[8]Vascular Biology Center, Department of Cellular Biology and Anatomy, Medical College of Georgia, Augusta University, Augusta, GA 30912, USA;

[9] Research, Central Texas Veterans Health Care System and [10] Department of Medical Physiology, Texas A&M University College of Medicine, Temple, TX 76504

*, equal contribution;

† Contact information

Chaodong Wu, MD, PhD, College Station, TX 77843, Email: cdwu@tamu.edu; or Gianfranco Alpini, PhD, Temple, TX 76504, E-mail: galpini@tamu.edu

Supplementary Information

MATERIALS AND METHODS

Animal experiments

Stimulator of interferon genes (STING)-disrupted ($STING^{gt}$) (C57BL/6J background) mice and wild-type (WT) C57BL/6J mice were obtained from Jackson Laboratory (Bar Harbor, ME). All mice were maintained on 12:12-h light-dark cycles (lights on at 06:00). **Study 1**: male WT C57BL/6J mice, at 5 - 6 weeks of age, were fed a high-fat diet (HFD, 60% fat calories, 20% protein calories, and 20% carbohydrate calories) or low-fat diet (LFD, 10% fat calories, 20% protein calories, and 70% carbohydrate calories) for 12 weeks. Additional male WT mice, at 11 - 12 weeks of age, were fed a methionine-and choline-deficient diet (MCD) or maintained on a standard chow diet for 5 weeks. After the feeding period, mice will be harvested to examine liver signaling events downstream of STING in relation to diet-induced non-alcoholic fatty liver disease (NAFLD) and/or non-alcoholic steatohepatitis (NASH). **Study 2**: male $STING^{gt}$ mice and WT mice, at 5 - 6 weeks of age, were fed an HFD for 12 weeks to examine a role for STING in NAFLD. Age-matched male $STING^{gt}$ mice and WT mice were fed an LFD for 12 weeks and served as controls. **Study 3**: male WT mice, at 5 - 6 weeks of age, were lethally irradiated and subjected to bone marrow transplantation (BMT) with bone marrow cells from $STING^{gt}$ mice and WT mice and designated as WT/BMT-$STING^{gt}$ mice and WT/BMT-WT mice, respectively, as described [1-3]. After recovery for 4 weeks, WT/BMT-$STING^{gt}$ mice and WT/BMT-WT mice were fed an HFD for 12 weeks as described in Study 2. **Study 4**: male $STING^{gt}$ mice, at 5 - 6 weeks of age, were lethally irradiated and transplanted with bone marrow cells from WT mice and $STING^{gt}$ mice and designed as $STING^{gt}$/BMT-WT mice and $STING^{gt}$/BMT-$STING^{gt}$ mice,

respectively. After recovery for 4 weeks, the chimeric mice were fed an HFD for 12 weeks. **Study 5**: male STING^{gt} mice and WT mice, at 11 - 12 weeks of age, were fed an MCD for 5 weeks. Age-matched male STING^{gt} mice and WT mice were maintained on a chow diet for 5 weeks and served as controls. All diets are products of Research Diets, Inc (New Brunswick, NJ). Detailed information of diet composition was included in Supplemental Table S1. During the feeding period, body weight of the mice was monitored weekly. Also, food amount was recorded weekly and used to calculate food consumption. After the feeding period, the mice in Studies 1 through 5 were fasted for 4 hr before sacrifice for collection of blood and liver samples. Livers were dissected and weighed as described [4-7]. Immediately after weighing, livers were either fixed and embedded for histological and immunohistochemical analyses or frozen in liquid nitrogen and stored at - 80 °C. Some mice were fasted similarly and used for insulin and glucose tolerance tests as described [4, 5, 8]. Prior to harvest, mice in Studies 2 through 4 were subjected to EchoMRI (EchoMRI LLC, Houston, TX) to analyze body composition. Also, some mice in Study 2 were subjected to the Promethion^{TM} system (Sable Systems International, North Las Vegas, NV) to measure energy metabolism. All study protocols were reviewed and approved by the Institutional Animal Care and Use Committee of Texas A&M University.

Human liver samples

Liver sections of human subjects with or without NAFLD were generated from donated tissues by Sekisui-XenoTech, LLC (Kansas City, KS, USA). Subjects were Caucasian males aged between 32 and 70 (NAFLD, 48.0 ± 14.8; non-NAFLD, 44.7 ± 10.6). Subjects with NAFLD revealed severe hepatic steatosis compared with subjects without NAFLD (44.7 ± 10.6% fat content vs. 1.7 ± 1.9%, assessed by XenoTech and by a board-certified pathologist (Dr. Xiangbai

Chen, Baylor Scott & White Health, College Station, TX 77845)). Because of using fixed human tissues that are commercially available, the current study was exempted from the Institutional Review Board (IRB) approval.

Histological and immunohistochemical analyses

Paraffin-embedded mouse liver blocks were cut into sections of 5 µm thickness and stained with H&E and/or stained for F4/80 expression with rabbit anti-F4/80 antibodies (1:100) (AbD Serotec, Raleigh, NC). Also, liver sections from Study 5 were stained with Trichrome to examine the status of liver fibrosis. Similarly, human liver sections were stained for H&E and/or Trichrome. Additional human liver sections were stained for STING expression using rabbit polyclonal antibodies against STING (Cat# 19851-1-AP) (Proteintech Group, Inc, Rosemont, IL, USA).

Measurement of plasma parameters

The levels of alanine aminotransferase (ALT) were measured using a metabolic kit (BioVision, Inc., Milpitas, CA). The levels of plasma glucose were measured using a metabolic assay kit (Sigma, St. Louis, MO). The levels of plasma triglycerides were measured using a biochemical assay kit (Wako Diagnostics, Richmond, VA).

Analysis of *in vivo* macrophage polarization

Stromal vascular cells (SVC) were isolated from epididymal fat depots of HFD-STING^{gt} mice and HFD-WT mice using the collagenase digestion method [9, 10]. The isolated SVC were assayed for macrophage subsets using BD Accuri™ C6 Plus flow cytometer (BD Biosciences, San Jose,

California, USA) as previously described [1, 11]. Among living cells, mature macrophages ($F4/80^+$ $CD11b^+$ cells) were gated for CD11c and CD206 expression (macrophage polarization). $F4/80^+$ $CD11b^+$ $CD11c^+$ $CD206^-$ cells were considered as proinflammatory (M1) macrophages whereas $F4/80^+$ $CD11b^+$ $CD11c^-$ $CD206^+$ cells were considered as alternatively activated (M2) macrophages.

Cell culture and treatment

Bone marrow cells were prepared from free-fed $STING^{gt}$ mice and WT mice, and differentiated into macrophages (BMDM) as described [1, 7]. Briefly, bone marrow cells were isolated from the tibias and femurs of the mice and differentiated in Iscove's modified Dulbecco's medium (IMDM) containing 10% fetal bovine serum (FBS) and 15% L929 culture supernatant for 6 - 8 days. After differentiation, BMDM were subjected to inflammatory assays and co-culture studies. To functionally validate STING disruption, $STING^{gt}$ and WT BMDM were treated with 5,6-dimethylxanthenone-4-acetic acid (DMXAA, 75 μg/mL) or control (7.5% $NHCO_3$) for 6 hr, and assayed for the levels of interferon beta (IFNβ) in macrophage-conditioned media using an ELISA kit (Catalog number: 424001, Invitrogen™, Thermo Fisher Scientific Inc., Waltham, MA USA). To analyze macrophage proinflammatory signaling, $STING^{gt}$ and WT BMDM were treated with DMXAA (75 μg/mL) or control for 24 hr in the absence or presence of lipopolysaccharide (LPS) (100 ng/mL, dissolved in 1× phosphate-buffered saline (PBS)) for the last 30 min to harvest cell lysates or LPS (20 ng/mL) for the last 6 hr to harvest RNA samples as described [7]. Also, the conditioned media of control- or DMXAA-treated $STING^{gt}$ BMDM and/or WT BMDM were collected and used to treat primary hepatocytes or LX2 cells (cell lines of human hepatic stellate cells (HSCs)) as described below. To analyze macrophage M2 activation,

STING^{gt} and WT BMDM were treated with or without interleukin 4 (IL-4, 10 ng/mL) for 48 hr and examined for the expression of IL-1β and IL-6.

Primary hepatocytes were isolated from free-fed WT C57BL/6J mice as described [7]. After attachment, hepatocytes were further incubated in M199 supplemented with 10% FBS and 100 U/mL penicillin and 100 μg/mL streptomycin for 24 hr. For hepatocyte-macrophage co-culture study, bone marrow cells were prepared from STING^{gt} mice and WT mice at 6 days prior to hepatocyte isolation. After differentiation, BMDM were trypsinized and added to WT primary mouse hepatocytes at a ratio of 1:10 as described [7, 12]. Some hepatocytes were incubated in the absence of macrophages and served as the control. Both co-cultures and hepatocytes were incubated with fresh media for 48 hr and treated with DMXAA (75 μg/mL) or control in the presence palmitate (250 μM) for the last 24 hr and assessed for fat deposition. In complementary experiments, some primary hepatocytes were incubated in M199 mixed with conditioned media of STING^{gt} BMDM or WT BMDM (that had been treated with DMXAA (75 μg/mL) or control for 24 hr) at a 1:1 ratio for 48 hr in the absence or presence of LPS (100 ng/mL) for the last 30 min to examine inflammatory signaling or LPS (20 ng/mL) for 6 hr to quantify the expression of genes for fat metabolism and cytokines.

LX2 cells were obtained from ATCC (Manassas, VA, USA), and maintained in DMEM with 2% FBS. At 90% confluence, LX2 cells were treated with DMXAA (75 μg/mL) or control in the absence or presence of transforming growth factor beta 1 (TGFβ1) (8 ng/mL) for 24 hr. Additional LX2 cells were treated with DMXAA (75 μg/mL) or control in the absence or presence of TGFβ1 (2.5 ng/mL) for 48 hr. Cell lysates were examined for the phosphorylation

states and/or total amount of p38 and alpha smooth muscle actin (αSMA). Also, total RNA of the treated LX2 cells were examined for the expression of collagen (type I alpha 1) (Col1a1), αSMA, fibronectin (Fn), TGF1β, and peroxisome proliferator-activated receptor gamma (PPARγ). To address the effects of STING-driven macrophage factors on HSC activation, HSC-macrophage co-cultures were performed by adding WT and/or $STING^{gt}$ BMDM that were pre-treated with DMXAA (75 µg/mL) for 24 hr to LX2 cells at a 1:10 ratio. Prior to harvest, the co-cultures were treated with without TGFβ1 (2.5 ng/mL) for 48 hr. In complementary experiments, LX2 cells were incubated in DMEM mixed with conditioned media of control- or DMXAA-treated $STING^{gt}$ BMDM and/or WT BMDM at a 1:1 ratio in the absence or presence of TGFβ1 (2.5 ng/mL) for 48 hr. After the incubation/treatment period, co-cultures and/or LX2 cells were harvested and examined for HSC activation.

Measurement of liver triglyceride levels

Frozen livers were extracted and measured for triglyceride levels using an assay kit from Wako (Richmond, VA).

Measurement of hepatocyte fat deposition

Hepatocyte-macrophage co-cultures, as well as control primary hepatocytes were treated with or without palmitate for 24 hr. At 1 hr prior to harvest, the cells were stained with oil red O and quantified for fat content as described [5, 7].

Molecular assays

To determine inflammatory signaling, lysates of frozen livers or cultured cells were subjected to Western blot analysis to measure total amount and/or phosphorylation states of JNK p46 and NFκB p65 as described [7, 13]. To examine signaling events downstream of STING, some mouse liver lysates were subjected to Western blot analysis to measure total amount and phosphorylation states of TBK1 and/or IRF3. All primary antibodies were from Cell Signaling Technology (Danvers, MA, USA). The maximum intensity of each band was quantified using ImageJ software. Ratios of Pp46/p46 and Pp65/p65, as well as P-TBK1/TBK1 and P-IRF3/IRF3 were normalized to GAPDH and adjusted relative to the average of LFD-fed control, HFD-fed WT control, HFD-fed WT/BMT-WT, HFD-fed $STING^{gt}$/BMT-$STING^{gt}$, MCD-fed WT, or PBS-treated control, which was arbitrarily set as 1 (AU). To examine gene expression, the total RNA was isolated from frozen tissues and cultured/isolated cells, and subjected to reverse transcription and real-time PCR analysis. Results were normalized to 18s ribosomal RNA and plotted as relative expression to the average of LFD-fed control, HFD-fed WT control, HFD-fed WT/BMT-WT, HFD-fed $STING^{gt}$/BMT-$STING^{gt}$, MCD-fed WT, or control cells with or without LPS treatment, which was set as 1.

REFERENCES

1. **Xu H**, **Li H**, **Woo S-L**, et al. Myeloid cell-specific disruption of Period1 and Period2 exacerbates diet-induced inflammation and insulin resistance. J Biol Chem 2014;289:16374-16388.
2. Delia B, Beatriz AB, Fengjie H, et al. Expression of microRNA-155 in inflammatory cells modulates liver injury. Hepatology 2018;0.

3. **Tian L**, **Changzheng L**, **Guizhi Y**, et al. Sphingosine kinase 1 promotes liver fibrosis by preventing miR-19b-3p-mediated inhibition of CCR2. Hepatology 2018;0.
4. Huo Y, Guo X, Li H, et al. Disruption of inducible 6-phosphofructo-2-kinase ameliorates diet-induced adiposity but exacerbates systemic insulin resistance and adipose tissue inflammatory response. J Biol Chem 2010;285:3713-3721.
5. **Huo Y**, **Guo X**, **Li H**, et al. Targeted overexpression of inducible 6-phosphofructo-2-kinase in adipose tissue increases fat deposition but protects against diet-induced insulin resistance and inflammatory responses. J Biol Chem 2012;287:21492-21500.
6. Woo S-L, Xu H, Li H, et al. Metformin ameliorates hepatic steatosis and inflammation without altering adipose phenotype in diet-induced obesity. PLoS ONE 2014;9:e91111.
7. **Cai Y**, **Li H**, **Liu M**, et al. Disruption of adenosine 2A receptor exacerbates NAFLD through increasing inflammatory responses and SREBP1c activity. Hepatology 2018;68:48-61.
8. **Guo X**, **Li H**, Xu H, et al. Palmitoleate induces hepatic steatosis but suppresses liver inflammatory response in mice. PLoS ONE 2012;7:e39286.
9. Lumeng CN, DeYoung SM, Bodzin JL, et al. Increased inflammatory properties of adipose tissue macrophages recruited during diet-induced obesity. Diabetes 2007;56:16-23.
10. Stienstra R, Duval C, Keshtkar S, et al. Peroxisome proliferator-activated receptor γ activation promotes infiltration of alternatively activated macrophages into adipose tissue. J Biol Chem 2008;283:22620-22627.

11. Wentworth JM, Naselli G, Brown WA, et al. Pro-inflammatory CD11c+CD206+ adipose tissue macrophages are associated with insulin resistance in human obesity. Diabetes 2010;59:1648.

12. **Odegaard JI**, **Ricardo-Gonzalez RR**, Red Eagle A, et al. Alternative M2 activation of Kupffer cells by PPARδ ameliorates obesity-induced insulin resistance. Cell Metab 2008;7:496-507.

13. **Guo T**, **Woo S-L**, Guo X, et al. Berberine ameliorates hepatic steatosis and suppresses liver and adipose tissue inflammation in mice with diet-induced obesity. Sci Rep 2016;6:22612.

Author names in bold designate shared co-first authorship.

Supplemental Table S1

Table 1. Diet composition

	LFD		HFD		CD	
	g%	kcal%	g%	kcal%	g%	kcal%
Casein, Lactic, 30 Mesh	18.96	19.72	25.84	19.72	20.00	20.71
L-Cystine	0.28	0.30	0.39	0.30	0.00	0.00
DL-Methionine	0.00	0.00	0.00	0.00	0.30	0.31
Corn Starch	47.98	49.91	0.00	0.00	15.00	15.54
Maltodextrin (Lodex 10)	11.85	12.31	16.15	12.32	0.00	0.00
Sucrose	6.9	7.18	9.4	7.17	50.00	51.79
Cellulose	4.74	0.00	6.46	0.00	5.00	0.00
Soybean Oil	2.37	5.55	3.23	5.55	0.00	0.00
Corn Oil	0.00	0.00	0.00	0.00	5.00	11.65
Lard	1.90	4.44	31.66	54.35	0.00	0.00
Total	94.98	99.41	93.13	99.95	95.3	100